Bio-Design and Manufacturing (2020) 3:266–280
https://doi.org/10.1007/s42242-020-00073-9

REVIEW

Heart-on-chips screening based on photonic crystals

Yixuan Shang[1] · Zhuoyue Chen[2] · Zhuohao Zhang[2] · Yuzhi Yang[1] · Yuanjin Zhao[1,2]

Received: 16 March 2020 / Accepted: 8 April 2020 / Published online: 23 April 2020

Abstract

Recently, organ-on-chips have become a fast-growing research field with the widespread development of microfluidic chips and synthetic materials in tissue engineering. Due to the existing cardiotoxicity of many cardiovascular drugs, heart-on-chips which are promising to replace traditional animal models have been extensively researched and developed to mimic human organ functions in vitro. The heart-on-chips mainly focus on cardiac mechanics, which is regarded as the central indicator of in vitro heart models and drug testing. Traditional methods for the detection of myocardial mechanics have been demonstrated complex and inefficient in heart-on-chips. Therefore, photonic crystal materials with unique optical properties have attracted interests and have been introduced into the heart-on-chips, developing a visualized self-reporting system for cardiomyocytes activity monitoring. In this review, photonic crystal-based heart-on-chips for biosensing are introduced, as well as the fabrication methods and design criteria of them. The characterizations of the photonic crystal materials are classified into optical properties and structural properties, and their applications in cell culture and biosensing are further discussed. Then, several representative examples and developments of the integration of photonic crystal materials into microfluidic chips are described in detail. Finally, potentials and limitations are put forward to promote the development of the photonic crystal-based intelligent heart-on-chips.

Keywords Heart-on-chip · Photonic crystal · Self-reporting · Biosensor · Drug testing

Introduction

Organs-on-a-chip, a type of microengineered biomimetic system, is fabricated based on microfluidic chips to imitate the critical functional units of living human organs in vitro [1–5]. Heart-on-a-chip is one of the examples and has received extensive attention as a potential solution to cardiotoxic side effects. The cardiac toxicities even exist in some FDA-approved cardiovascular disease drugs, so that the heart-on-chips are expected to achieve the drug toxicity screening partly replacing the in vivo experiment [6–8]. In the researches of cardiac disease modeling and drug testing, various methods have been presented to measure myocardial contractility, which is regarded as the key functional assessment parameters of the heart-on-chips [9–13]. These methods include microelectrode arrays, micropillars, microcantilevers hydrogel thin films embedded with fluorescent beads and so on [14–18], which have made progress in myocardial contraction detection. However, most existing strategies are unintuitive and highly time-consuming, so that there is still a demand for the development of operable systems with efficient biosensors and visual feedback.

Photonic crystals (PhCs) have been extensively studied for decades due to their miraculous optical properties. The PhC is a kind of periodic dielectric structure with photonic bandgaps (PBGs). According to the effect of Bragg diffraction, PhCs possess adjustable lattice and angle-dependence properties, which could respond to deformation such as bending or stretching by PBG shifts [19–21]. These characteristics impart PhCs with great technological significance in self-reporting biosensors [22–26]. Therefore, many PhC materials have been utilized as substrates and embedded in the heart-on-chips for self-reporting force sensing.

✉ Yuzhi Yang
yangyuzhi5500@163.com

✉ Yuanjin Zhao
yjzhao@seu.edu.cn

1 Department of Clinical Medical Engineering, Nanjing Drum Tower Hospital, The Affiliated Hospital of Nanjing University Medical School, Nanjing 210008, China

2 State Key Laboratory of Bioelectronics, School of Biological Science and Medical Engineering, Southeast University, Nanjing 210096, China

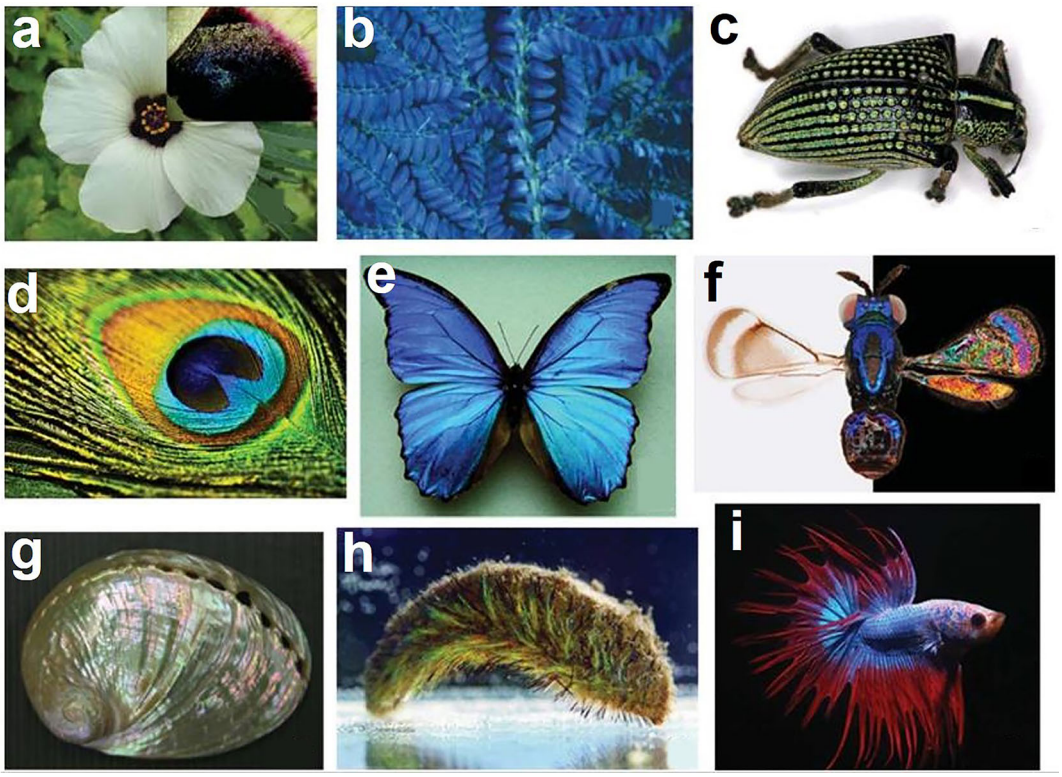

Fig. 1 PhCs in the biological world. **a** Base of *H. trionum* petal; **b** the fern-like tropical understory plants of the genus *Selaginella*; **c** the diamond weevil beetle, *Entimus imperialis*; **d** the male peacock's tail feathers; **e** the blue butterfly *Morpho rhetenor*; **f** the *Clostero-cerus coffeellae* (Hymenoptera insect); **g** the nacre of *Haliotis glabra*; **h** *Aphrodita aculeata* (a species of sea mouse); **i** siamese fighting fish [29]

In this review, we introduce the general processing methods of PhC materials in the biomedical field, including the modification of natural PhCs and synthesis of artificial PhCs. Then, we focus on the characterization of the PhC materials, including optical properties, specific cell inductivity and applied potentials in tissue engineering and biosensors. Examples of representative PhC materials integrated into microfluidic chips are presented in detail, such as their microfabrication, cardiomyocytes culture, visual detecting and the specific analysis of myocardial contraction. Finally, we propose a general summary and put forward a prospect for the future development of the PhC-based intelligent heart-on-chips.

Generations of PhC materials

Typical examples of natural PhCs

Scientific studies of PhCs initiated in the late 1980s, and the concepts were almost simultaneously proposed by Yablonovitch [27] and John [28]. The PhC is a kind of optical materials, in which more than two dielectric media with different refractive indexes and dielectric constants are arranged periodically. Due to these microstructures, the PhCs can manipulate the propagation of light (or photons) in their PBGs, thereby exhibiting bright structural colors. Gem opals are natural PhC materials, which are the formation of ordered sedimentation of silica nanoparticles after a long-lasting siliceous deposition and concentration under fluid forces and gravity. In the biological world, various natural creatures are possessing PhCs, such as insects, birds, mollusks, sea mice, fish and some plants [29]. With bright structural colors, these natural creatures present coloration variations through PhC structural changes for camouflage, predation, signal communication and sex choice (Fig. 1).

Assembling of artificial PhCs

Assembling of PhC films

Inspired by the natural examples, a variety of synthetic PhC materials with glaring structural colors have been designed in forms of films, particles and fibers via diverse approaches. Generally, the synthetic PhC films were fabricated by the bottom–up assembly of monodisperse colloidal particles [30,

31]. When the construction units of colloidal particles and the derived PBGs couple with the wavelength ranged in visible light, the synthetic PhC films will display unique visible optical properties. To fabricate the PhC films, there are two assembly methods according to the properties of colloidal particles: the close-packed arrays and the non-close-packed arrays. Among them, PhC films based on close-packed arrays and their derivatives have demonstrated their potential in manufacturing and biosensing.

As the most widespread approach, the vertical deposition method is widely used for the preparation of close-packed PhC films [32–34]. In the fabricating process, the substrate is firstly immersed vertically into a monodispersed colloidal particle solution, and then the colloidal solution is volatilized to lower the meniscus level. At the beginning of the deposition, the colloidal particles stay at the menisci region contacting with the substrate and adhere onto the substrate with liquid-level drawdown, and other colloidal particles gradually move and stick to the immobile particles. As the solvent evaporates, the monodispersed colloidal particles are orderly assembled on the substrate to form a brilliant PhC films. The assembly of colloidal particles is usually affected by factors such as the evaporation rate of the solvent and the concentration of colloidal particles, which would result in structured defects. To solve this issue and achieve larger monomorphic regions and tractable thickness, Jiang and Yang developed an adjustable doctor blade coating method. Firstly, monodisperse silica microparticles were dispersed in an involatile monomer ethoxylated trimethylolpropane triacrylate (ETPTA) with 2 wt% photoinitiator, and an immobilized beveled razor blade was vertically placed to gently touch with the substrate. Then, dragged with a syringe pump, the substrate moved with controllable speed and was sheared by a razor blade. Finally, the substrate covered with the ETPTA monomer was exposed in the ultraviolet radiation and transformed into 3D highly ordered colloidal crystal–polymer nanocomposites [35]. Besides, Gu et al. [36] proposed a novel pull-up deposition method, in which the substrate was immersed in a monodisperse colloidal particle solution and lifted at a certain speed to obtain a uniform thickness of PhC film with higher productivity. Benefiting from the exquisite preparation technologies, PhC films with unique optical properties have been successfully developed and widely applied in the field of optical biosensing (Fig. 2).

Assembling of PhC beads

PhC beads are essentially spherical colloidal crystal clusters. Similar to the PhC films, close-packed and non-close-packed are two assembly methods for PhC beads [37]. During the preparation of the close-packed beads [38], the colloidal particles are firstly dispersed into droplet templates and dried to evaporate the solvent, thus facilitating the particles assembling into colloidal crystal clusters (Fig. 3a). Recently, microfluidic emulsification technologies have provided a novel method for assembling PhC beads and special beads, and the size or structural color of the beads could be precisely controlled by varying the flow rate of fluid phases or the size of colloidal particles [39–41]. Zheng et al. presented a type of barcode particles which could synchronously capture, detect and release various circulating tumor cells from a composite sample [42]. They fabricated barcode particles with microfluidic technology, and the surface of the barcode particles was etched with a hydroxide solution to achieve tightened and aligned surfaces with non-closed-parked nanostructures. The unique particles enabled probe immobilization and cell adhesion, providing a nanopatterned platform for highly efficient bioreactions (Fig. 3b). In addition, non-close-packed PhCs could also be directly produced by microfluidic technology [37, 43]. The difference was the usage of surface-charged particles in droplet templates. The high-concentration charges would create repulsion between the particles, and the minimum energy configuration led the colloidal particles self-assemble into a non-close-packed face-centered cube (FCC). Furthermore, researchers dispersed charged particles in a medium with high-purity nonionic hydrogel monomers, locking the colloidal particles by the cross-linked hydrogel network structure, and regulated the structural color by changing the concentration of colloidal particles (Fig. 3c). This breakthrough ensured the stability of PhC beads and expanded the application of PhC beads in intelligent optical sensors [44].

Fabrication of inverse opals

These self-assembled PhC materials possess nearly 26% voids among the colloid particles, which contributes to the PhC materials acting as templates for the filling of diverse materials; hence, self-assembled PhC materials are often referred as “colloidal crystal templates” [30]. Specifically, the colloidal crystal templates are infiltrated and covered with solid-, liquid- or gas-phase prepolymers and are subsequently removed by calcining, dissolving or chemical etching after polymerization to acquire porous materials with highly ordered and interconnected spherical voids [45–47] (Fig. 4). The obtained porous materials, usually called inverse opals, possess a large specific surface area, interpenetrating pore channels, high pore volume and high drug loading capacity, which are conducive to cell adhesion and nutrient transmission, etc. In addition, inverse opals replicate the template lattice structures reversely and possess PBGs with corresponding optical features. The optical and structural properties, as well as the wide selection of multifunctional polymers, make inverse opals valuable in tissue engineering, biosensing and other fields [48, 49].

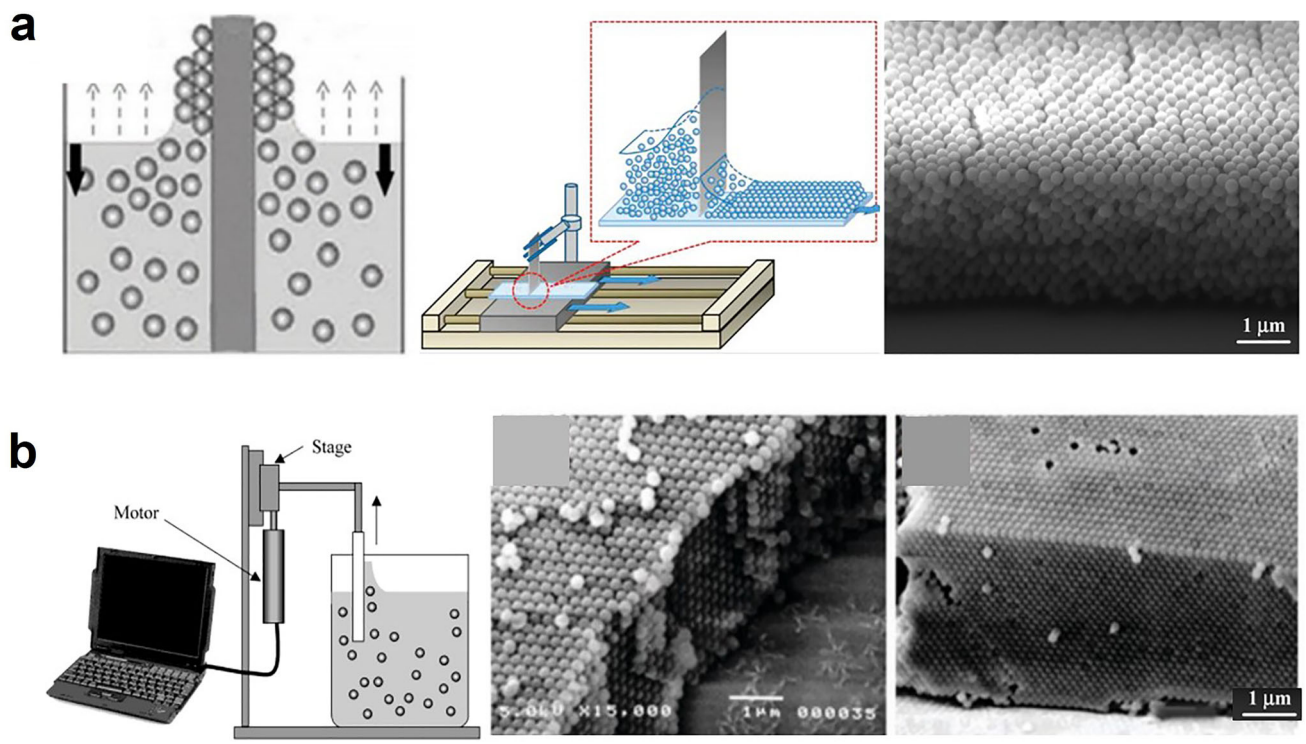

Fig. 2 **a** Schematic diagram of the vertical deposition method, the adjustable doctor blade coating technique and the cross-sectional SEM images of the resulting silica colloidal crystal [33, 35]; **b** outline of the pull-up deposition method and the cross-sectional SEM images of colloidal crystals [36]

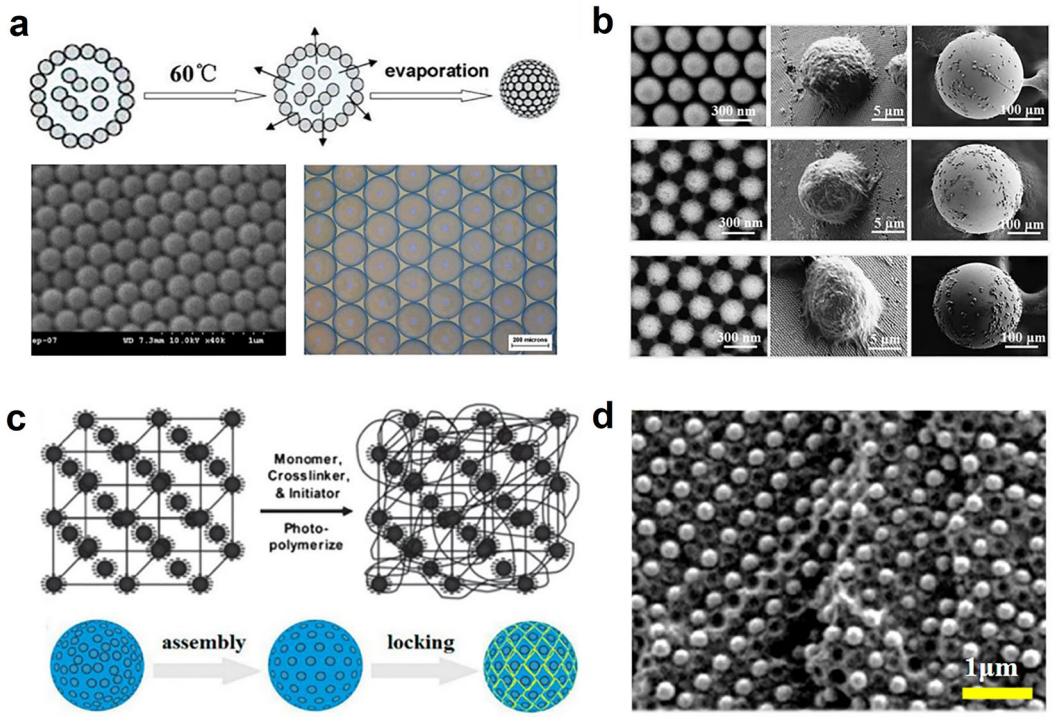

Fig. 3 **a** Fabrication and characterization of the close-packed colloidal PhC beads [38]; **b** SEM images of the surface nanostructure and the captured CTC of various barcode-particle substrates [42]; **c**, **d** generation and characterization of non-close-packed colloidal PhC beads [37]

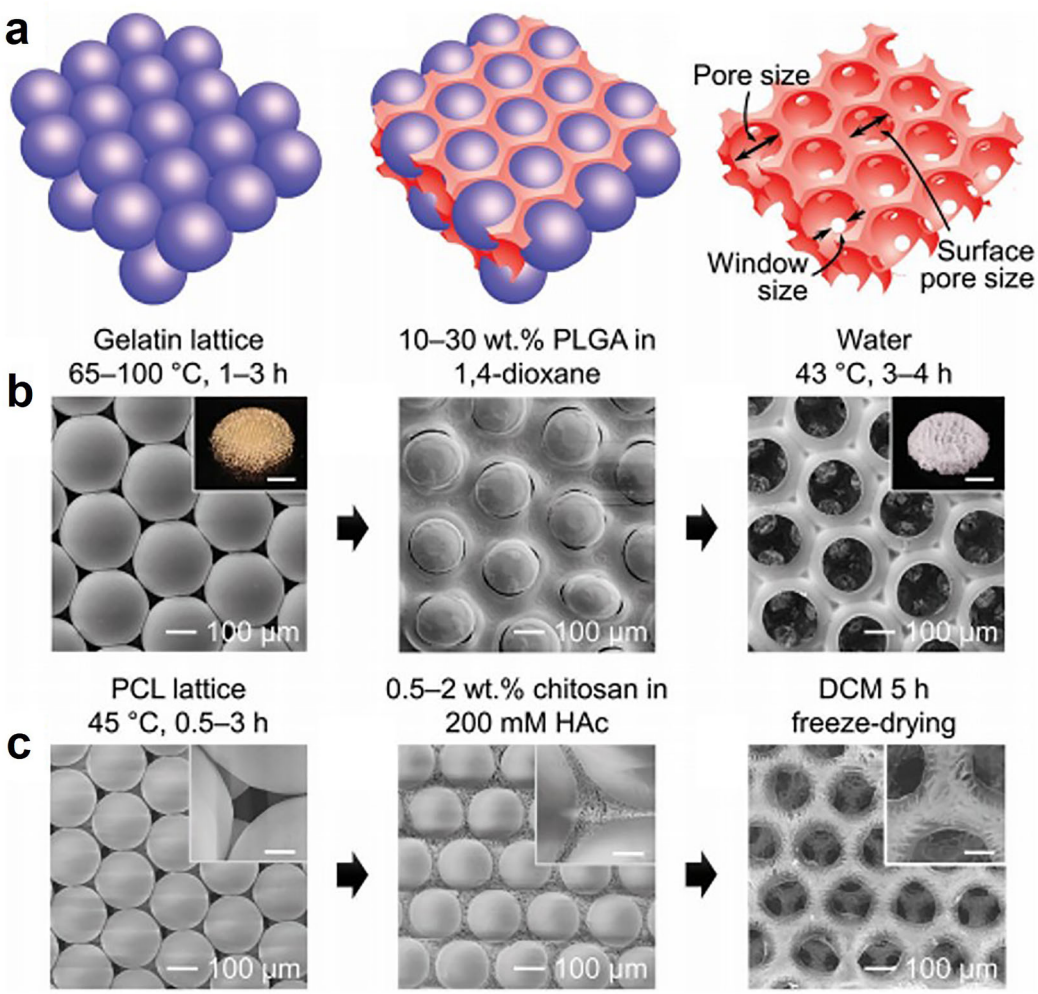

Fig. 4 **a** Schematic diagram exhibiting the fabrication of inverse opals [48]; **b**, **c** SEM images showing the fabrication of inverse opal scaffolds from uniform microspheres [45–47]

PhCs as normal biomaterials

Natural PhCs

As one of the best-studied PhCs in nature, butterflies with parallel nanoridges structured wing scales demonstrate the capabilities to control the photons propagating in the PBGs and thus display splendid structural colors [29]. The hierarchical structure mainly constituted by chitin not only leads to special optical features but also implies potentials in tissue engineering. It was confirmed that surface topography patterns with grooves or ridges possess the capability to induce cell orientation. Gu et al. utilized the ridge-structured *Morpho menelaus* (*M. menelaus*) butterfly wings as substrates for RSC96 cell growth [50]. After acidic and basic treatments, the *M. menelaus* wings became hydrophilic and induced cells into a regular alignment along with the ridges (Fig. 5a). Additionally, Elbaz et al. proved the coincident fibroblast orientation of butterfly wings with anisotropic nanostructures [51] (Fig. 5b). With remarkable effects on cell behaviors, the natural PhCs present a promising prospect in tissue engineering and motivate artificial fabrication.

Inverse opal films

Cell alignment plays a vital role in proliferation, differentiation, wound healing and even pathological processes, etc. [52–55]. Recently, various substrates with designed surface topology have been fabricated to regulate cell alignment [56–61]. In particular, inverse opal films have attracted notable research interest due to their specific periodic macroporous structure [62]. Gu et al. fabricated silica colloidal crystal templates by using a vertical deposition method and sintered the templates to strengthen the junction structures of adjacent particles [63]. Then, the polystyrene (PS)/toluene solution was infiltrated into the voids of the template to form the composite film after solvent evaporation. The template was subsequently etched by hydrofluoric acid to obtain

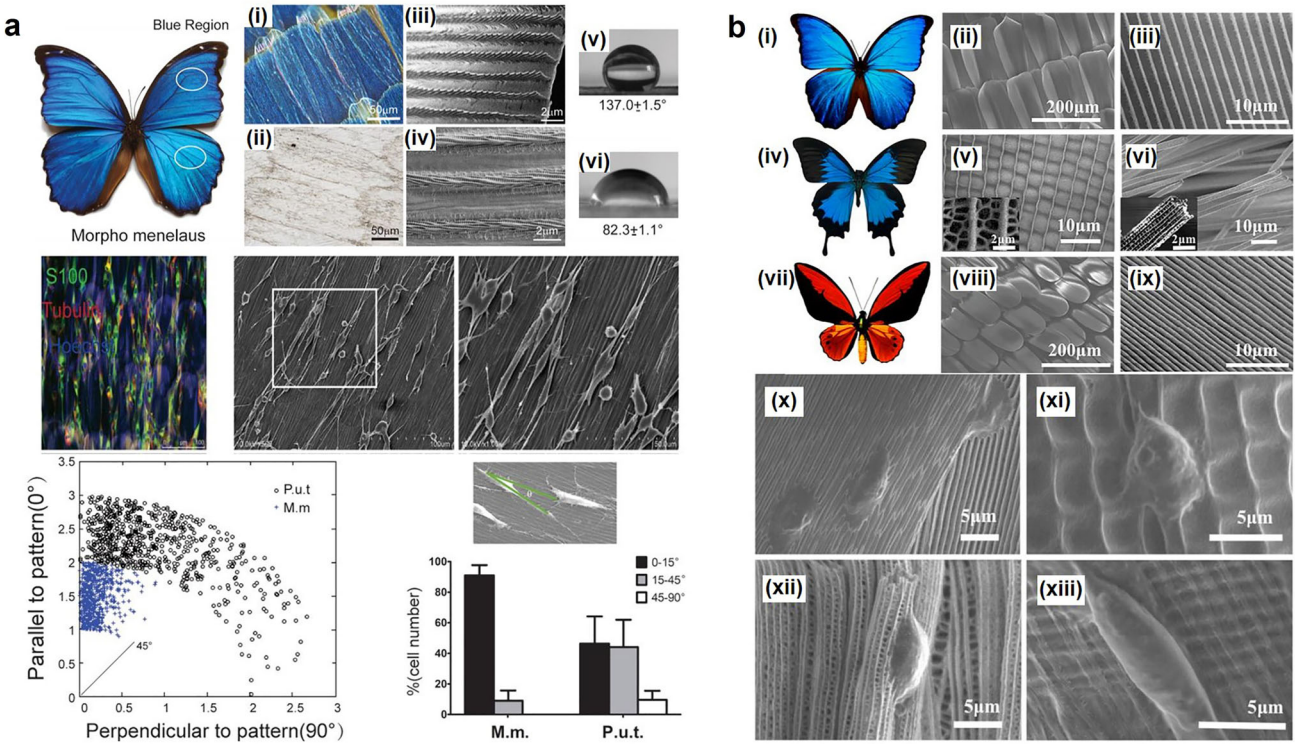

Fig. 5 **a** Characterization of the *M. menelaus* and the cells growing on the butterfly wings [50]; **b** characterization of the wings and the SEM images of cells after 48 h cultured on the wing [51]

the PS inverse opal film. Finally, the film with a gradient stretching ratio was acquired by repetitive uniaxial stretching via Vernier caliper at a temperature close to the glass transition temperature. They demonstrated that the elliptical topology derived from the stretched inverse opals could regulate different degrees of cell orientation. The cells growing on the maximum stretch part (12 times) presented an aligned orientation along the stretching direction, and the cell microfilaments were also elongated to the maximum to form tight cell–cell connections. In addition, they achieved random-to-aligned-oriented morphologies of cells on the gradient increased stretching inverse opal substrates without any chemical modifications, mimicking the insertion part of many connecting tissues and providing potential applications in tissue engineering (Fig. 6).

Inverse opal beads

Conventional drug delivery methods, such as systemic, local or oral delivery, may have strong side effects and uncontrolled drug concentration in the blood. Rejecting the disadvantages of traditional methods, the drug delivery system based on inverse opal beads demonstrated high control and high drug loading capacity, ensuring drug efficacy during drug release [64–67]. Liu et al. proposed a kind of egg-derived composite beads for synergistic drug delivery [68]. After reversely replicating the silica colloidal crystal templates, the egg yolk inverse opal beads were obtained with high surface areas and interpenetrating nanoholes. Then, the egg yolk beads were infiltrated into hydrophobic camptothecin solution to implement the first loading and immersed into the doxorubicin-dissolved egg white solution for the second sample loading. The compounded beads could exert the synergistic effect of the two drugs, obviously reduce cell viability and facilitate the therapeutic effect on hepatoma cells. The compounded beads were also used for a long-term cancer treatment, which was considered as a promising microcarrier for clinical drug delivery (Fig. 7a).

As typical synthetic PhCs, responsive inverse opal beads could be constructed by using stimulus-responsive materials [31, 69]. Wang et al. proposed hydrogel inverse opal beads with multi-functions, including maneuverable drug release, visual thermal/pH-double response and rapid cell viability detection [70]. They introduced *N*-isopropyl acrylamide (NIPAM) and acrylic acid (AA) into the hydrogel precursors, enabling the inverse opal beads to respond to changes in temperature and pH through definite volume change. In particular, inverse opal beads were endowed with PBGs and corresponding characteristic reflection peaks; thereby, the volume response could transform into the optical response. As expected, the results indicated that living H460 cells could secrete plenty of lactic acid in a doxorubicin-free

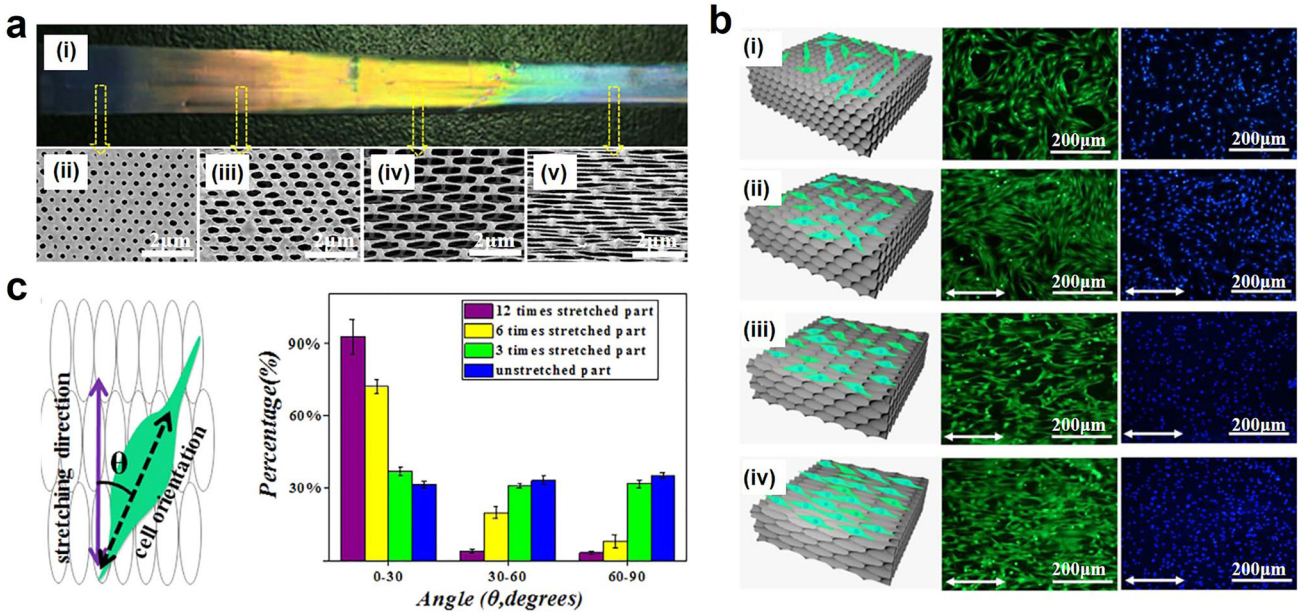

Fig. 6 **a** Optical and SEM images of the gradient stretched inverse opal film; **b** schematic diagram and fluorescence images of fibroblast cells cultured on the gradient stretched inverse opal film; **c** orientation angle frequency distribution of cells cultured on different part of the stretched inverse opal film [63]

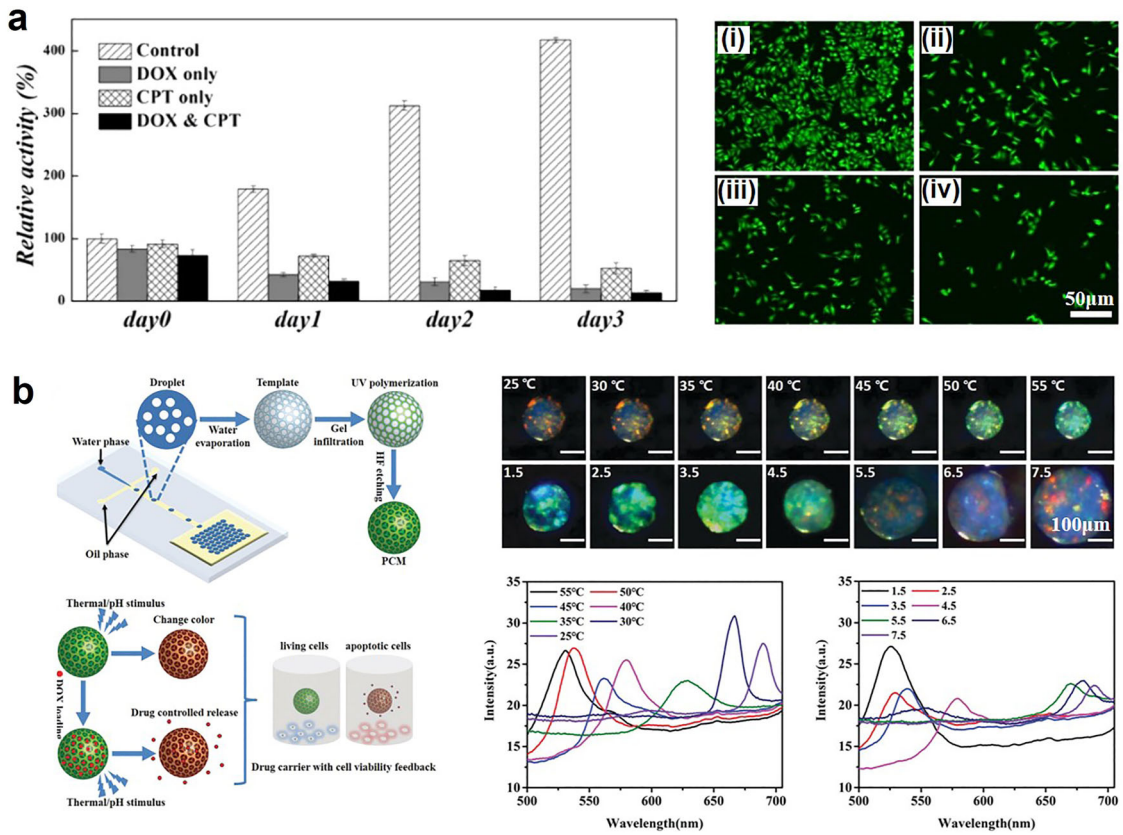

Fig. 7 **a** MTT assays and fluorescent images of the hepatoma cells after respective 3 days and 1 day of culture in the different groups to demonstrate the co-delivery of DOX and CPT in the egg component-composited beads [68]; **b** the fabrication diagram and responsiveness of the hydrogel inverse opal beads [70]

environment, and the resulting acidic environment regulated the color of inverse opal beads with a blue-shift turning to green. After the doxorubicin addition, a large number of cell apoptosis gave rise to a neutral microenvironment that accordingly caused the color of inverse opal beads shifting to red (Fig. 7b). These responsive inverse opal beads provided a visual detection of cell viability, laying the foundation for the construction of visualized drug screening systems.

PhC materials for heart-on-chips

Natural PhCs as self-reporting sensors

Heart-on-chips have aroused widespread attention as they present a new thought to simulate heart functions in vitro. The developments of cell monitoring and drug testing raise a great demand for advanced self-reporting technology, which gains increasing importance in heart-on-chips. PhC materials are highly promising to be utilized as substrates of heart-on-chips as their peculiar periodic structure and optical properties. Specifically, the natural PhC materials were accessible and their inherent topography and optical properties could induce cell behavior and report cell viability. For example, Chen et al. presented a self-reporting biosensor by assembling cardiomyocytes on the wings of the *M. Menelaus* [71]. The *M. Menelaus* wings were firstly modified by oxygen plasma to gain hydrophilic surface wettability, then filled with carbon nanotubes in the wing gaps to enhance conductivity and finally infiltrated with bioactive methacrylated gelatin (GelMA) hydrogel to obtain better biocompatibility and nutritional capacity. After planting cardiomyocytes on the wings, they presented that the assembled cardiomyocytes could recover autonomous rhythmic excitement without external stimulation and exhibit an ordered alignment responsive to the periodic parallel nanoridges of the wings. Accordingly, the soft butterfly wings could perceive and report cardiomyocyte beating with the same cycle of deformations and corresponding shifts in their structural color thus offered a visualized self-reporting for cardiomyocyte mechanics. Particularly, the cultured cardiomyocyte sources involved primary rat cardiomyocytes and induced pluripotent stem cells (iPSCs), and both of them gained self-report property on the *M. Menelaus* wings (Fig. 8). Therefore, the natural creatures, such as the *M. Menelaus*, are valuable for human physiological simulation and biomedical applications.

Artificial PhC films as self-reporting sensors

Artificial PhC films with anisotropic surface topography and potential visualization property have been fabricated and applied for the heart-on-chips system [72–74]. Comparing to conventional heart-on-chips, the one based on PhC films possesses self-reporting functions with visualized feedback of cellular force. Fu et al. assembled colloidal crystals on silicon wafers with microgroove patterns and used soft GelMA hydrogel to reversely replicate the hierarchical structure [72]. The microgrooves of the soft film could effectively induce cardiomyocytes orientation, and the periodic nanopores were sensitive to cardiomyocytes beating with the capability of transforming contraction force into visual signals. In addition, by integrating the soft films into the microfluidic chip, they developed a self-reporting heart-on-a-chip and provided a new tool for visualizable biological research and drug screening (Fig. 9).

In one of their subsequent studies, a reduced graphene oxide (rGO) hybrid film was composed of polyethylene glycol diacrylate (PEGDA), rGO-doped GelMA and the rGO film [73]. Because of the differences in biocompatibility, cardiomyocytes could only adhere to rGO-doped GelMA region and recover rhythmed beating, whereupon the adjacent PEGDA region was stretched with deformation and resulted in color shifts. The relationship between wavelength shifts and external strain could be analyzed quantificationally so that realizing the precise mechanical-to-optical conversion. Therefore, the rGO-doped composite film implemented the division of the function area for cell culturing and self-reporting sense, preventing the PBG structures disturbance caused by cell adhesion and growth. Particularly, as a material with remarkable electrical features, the rGO incorporated in the GelMA region would promote the electrical conductivity in cardiomyocytes and improve the beating consistency. This hybrid PhC film would provide a novel strategy for the further development of self-reporting biosensors (Fig. 10).

Despite these achievements, the microgrooves may divide cardiomyocytes into an isolated state, hindering researches on intercellular communication, interstitial connections and coordinated cellular effects. Therefore, Shang et al. [74] fabricated a flat inverse opal substrate with stretch-derived periodical elliptical macropores. Under the guidance of the anisotropic substrate, cardiomyocytes aligned along the stretching direction. Meanwhile, cell pseudopods could extend to the longest on the flat substrate and generated coherent intercellular junction. Similarly, they constructed visualized heart-on-chips based on this anisotropic substrate and achieved self-reporting cardiac activity sensing (Fig. 11).

PhC beads as self-reporting sensors

Since droplet microfluidics was extensively investigated for functional material synthesizing, PhC beads have found optimal avenues, which shed light on visual measuring systems [75–77]. Wang et al. developed a strategy for construct-

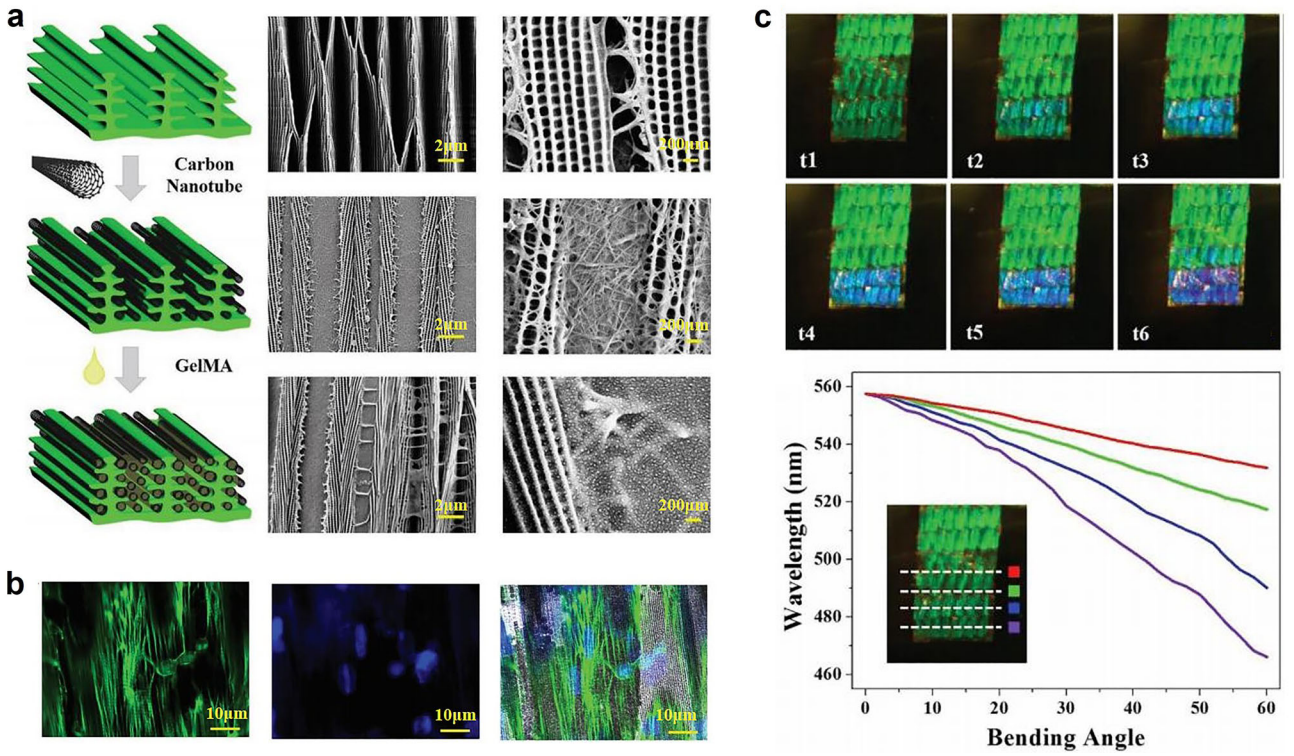

Fig. 8 **a** Modified scheme images and SEM images of the *M. Menelaus* wing scales; **b** fluorescence images of the cardiomyocytes cultured on the modified *M. Menelaus* wing scales; **c** the cardiomyocytes-actuated color changing process of the *M. Menelaus* wing [71]

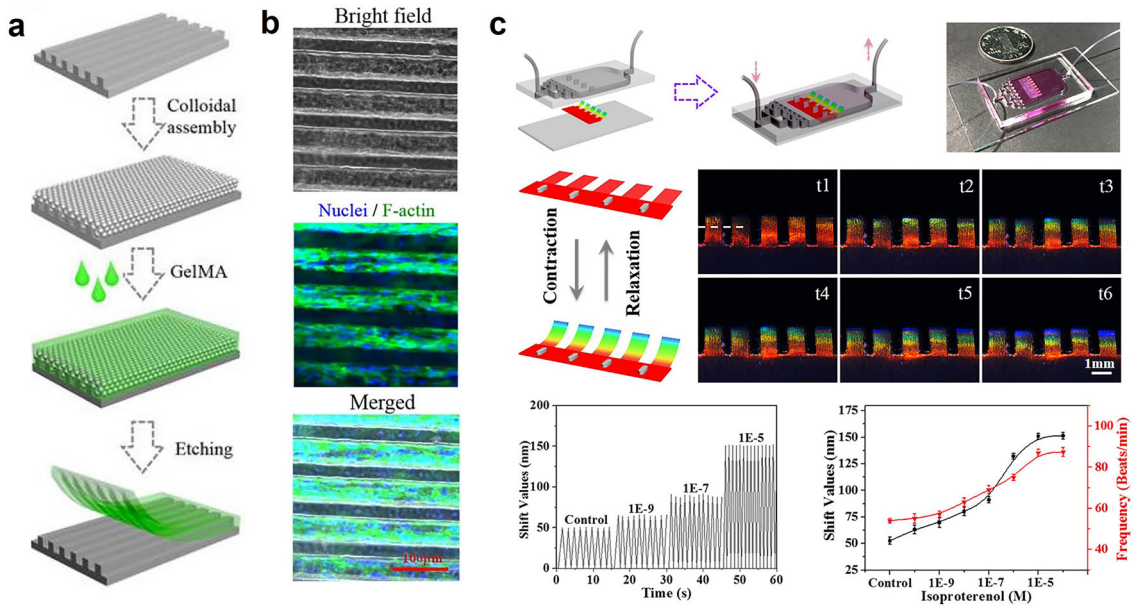

Fig. 9 **a** Schematic diagram of the generation process of the microgroove patterned hydrogel films; **b** fluorescence images of cardiomyocytes cultured on the microgroove patterned hydrogel film; **c** the applications of the soft films in a heart-on-a-chip system [72]

ing an anisotropic structural color bead by coassembling graphene oxide (GO) and silica nanoparticles in droplets [78]. As the water in the droplets evaporated, anisotropic Janus beads were assembled with hemispherical colloidal crystal aggregate and oblate GO layer. Then, these Janus beads were calcined in the argon protection environment to enhance mechanical strength, and meanwhile, the GO was reduced into rGO. They used the anisotropic Janus beads as

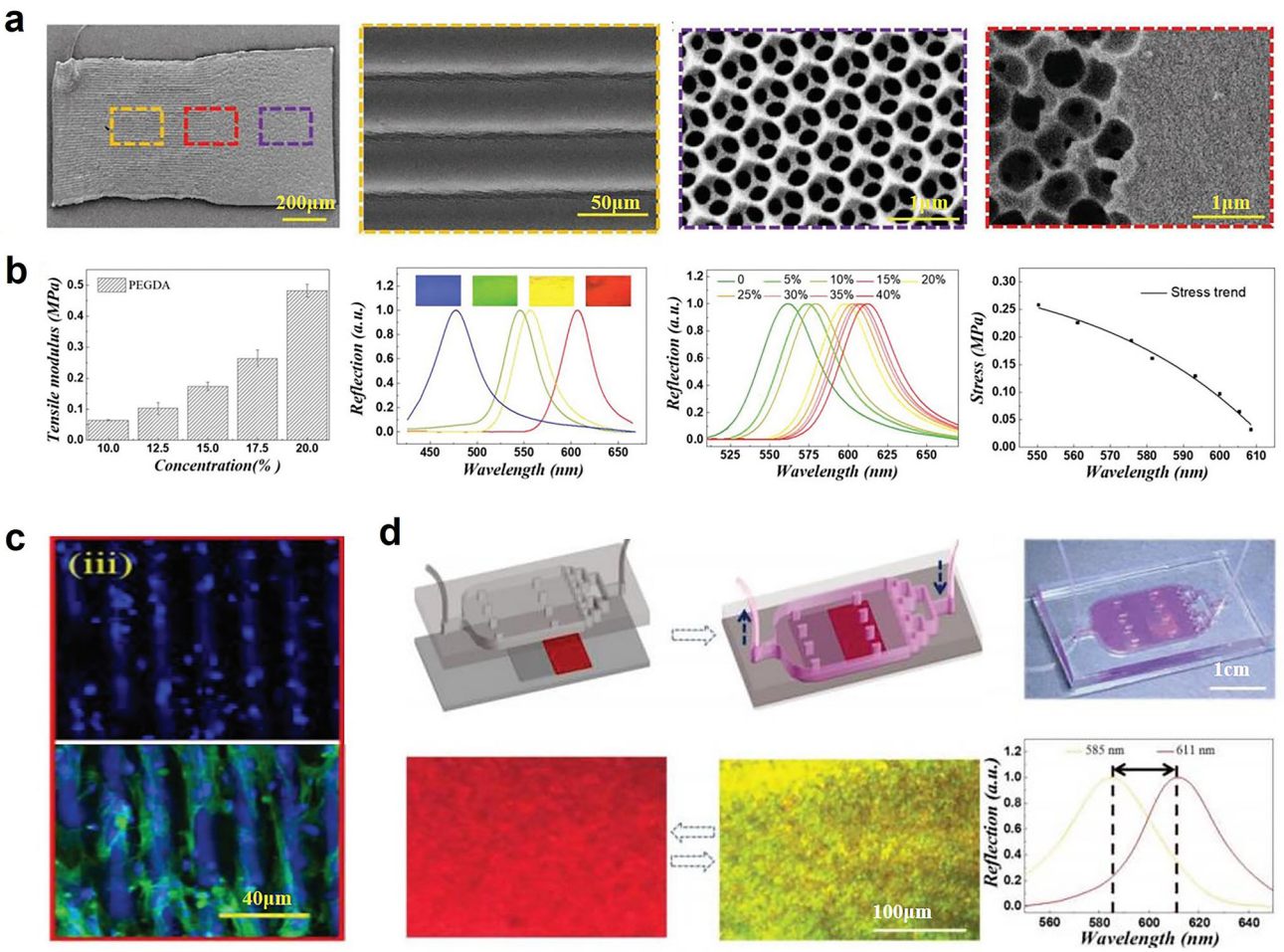

Fig. 10 **a** SEM images of the hybrid PhC film; **b** the reasoning process of the relationship between spectral reflection peak and external stress; **c** fluorescence images of the cardiomyocytes cultured on the hybrid PhC film; **d** the applications of the hybrid PhC film in a heart-on-a-chip system [73]

templates for constructing responsive structural color hydrogel beads. In this process, the GelMA pregel was firstly infiltrated into the voids of the anisotropic Janus beads. After irradiation with ultraviolet (UV) light, the solution was polymerized to acquire silica/rGO-GelMA hybrid beads, and the porous rGO-GelMA hydrogel beads were finally obtained by hydrofluoric acid etching. The hemispherical porous structure imparted the hydrogel beads with specific PhC properties, and the oblate rGO section enhanced the color contrast and provided a macroscopically fixable feature. Then, the hydrogel beads were used to culture and monitor cardiomyocytes (Fig. 12a). According to the results, about 20 cardiomyocytes, at single-cell level, were planted on a single hydrogel bead, while their beating could actuate the deformation and structural color shift of the hydrogel bead (Fig. 12b). Furthermore, the hydrogel beads realized drug testing of cardiomyocytes through visual feedback even accessible to the naked eye (Fig. 12c). Therefore, the real-time detection of the PhC beads is a promising method for visual single-cell monitoring and mechanical analysis.

PhCs self-reporting soft robots

Further, different from these mentioned fixed heart-on-chips, the biomimetic soft robot was utilized to measure myocardial mechanics via biomimetic motorial capabilities rather than structural color shifts of the fixed substrate. Sun et al. got inspiration from natural reptiles and designed a sophisticated soft robot with a structural color layer topside, an aligned carbon nanotube (CNT)-induced cardiomyocytes middle layer and unsymmetrical claws underneath [79]. With cell orientation inductivity and excellent conductivity, the aligned CNT layer facilitated cardiomyocytes to achieve consistent align-

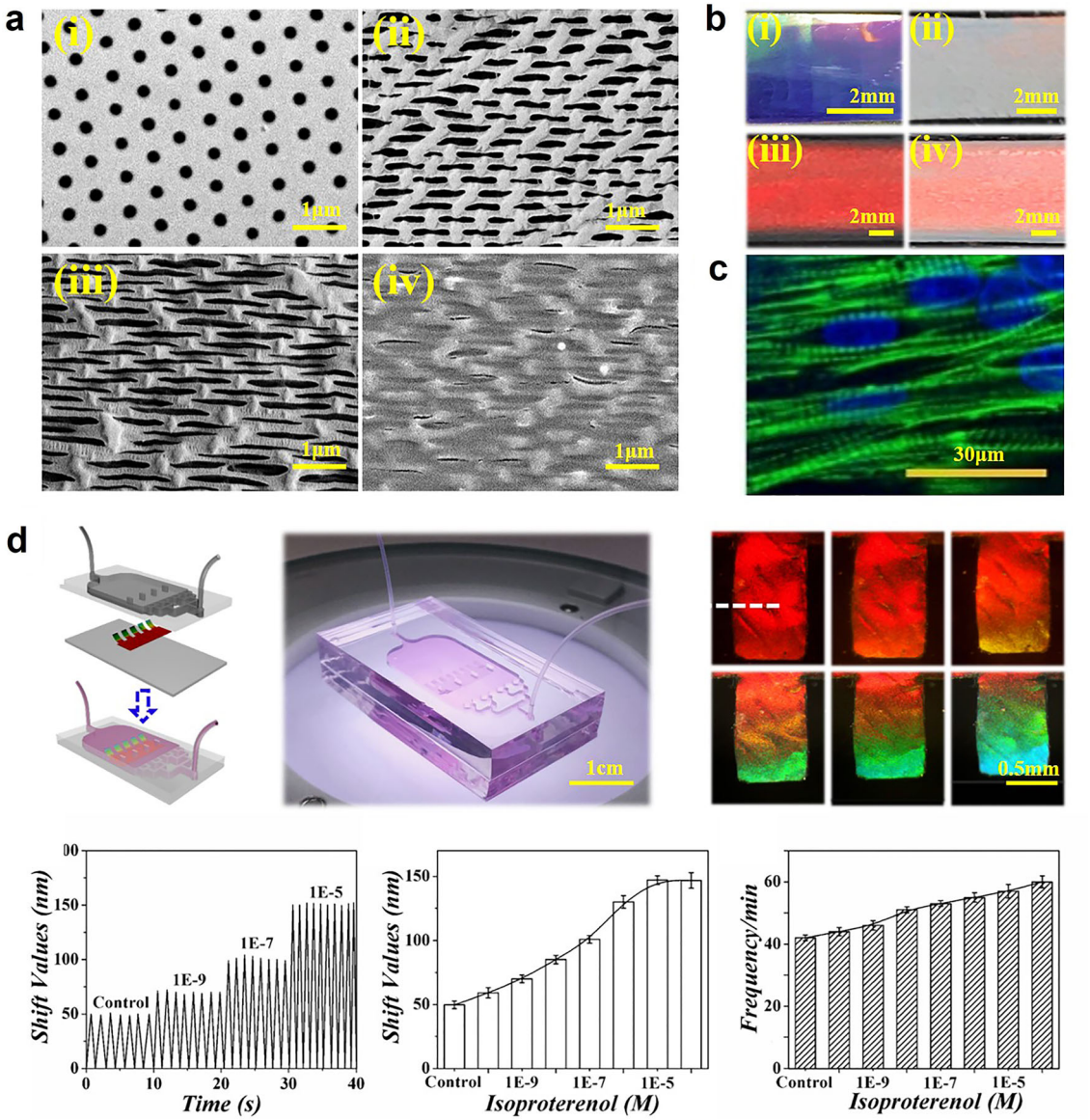

Fig. 11 **a** SEM images of the inverse opal substrates with different stretching degrees; **b** optical images of the inverse opal substrates with different stretching degrees; **c** fluorescence image of the cardiomyocytes cultured on the inverse opal substrate with 6 times stretching degree; **d** the applications of the inverse opal substrates in a heart-on-a-chip system [74]

ment and restore autonomic rhythmic beating. Benefiting from the design, the soft robot could crawl like a worm driven by cardiomyocytes and exhibited gorgeous structural color shift consistent with the cardiomyocyte beating. Finally, the soft robots were integrated into a microfluidic heart-on-chip system and showed different running speeds in response to different drug concentrations (Fig. 13). Therefore, this integrated system could intuitively evaluate cellular state by detecting the structural color shift and the running distance of soft robots, showing a simple evaluation platform for investigating drug tests and disease mechanisms.

Perspective and conclusion

The potential of the organ-on-chips is of great promotion for the development of disease models in vitro and drug test systems, owing to their conducive effect to the imitation of human-organ functions and the measurement of therapeutic drug effects. As one of organ-on-chips, heart-on-chips demonstrate the potential in researches about heart tissue engineering. The keys to the prosperity lie in the innovation in the methodologies and conditions for cardiomyocytes mechanical detecting. The major focus of the researchers is to improve the myocardial mechanical detecting methods

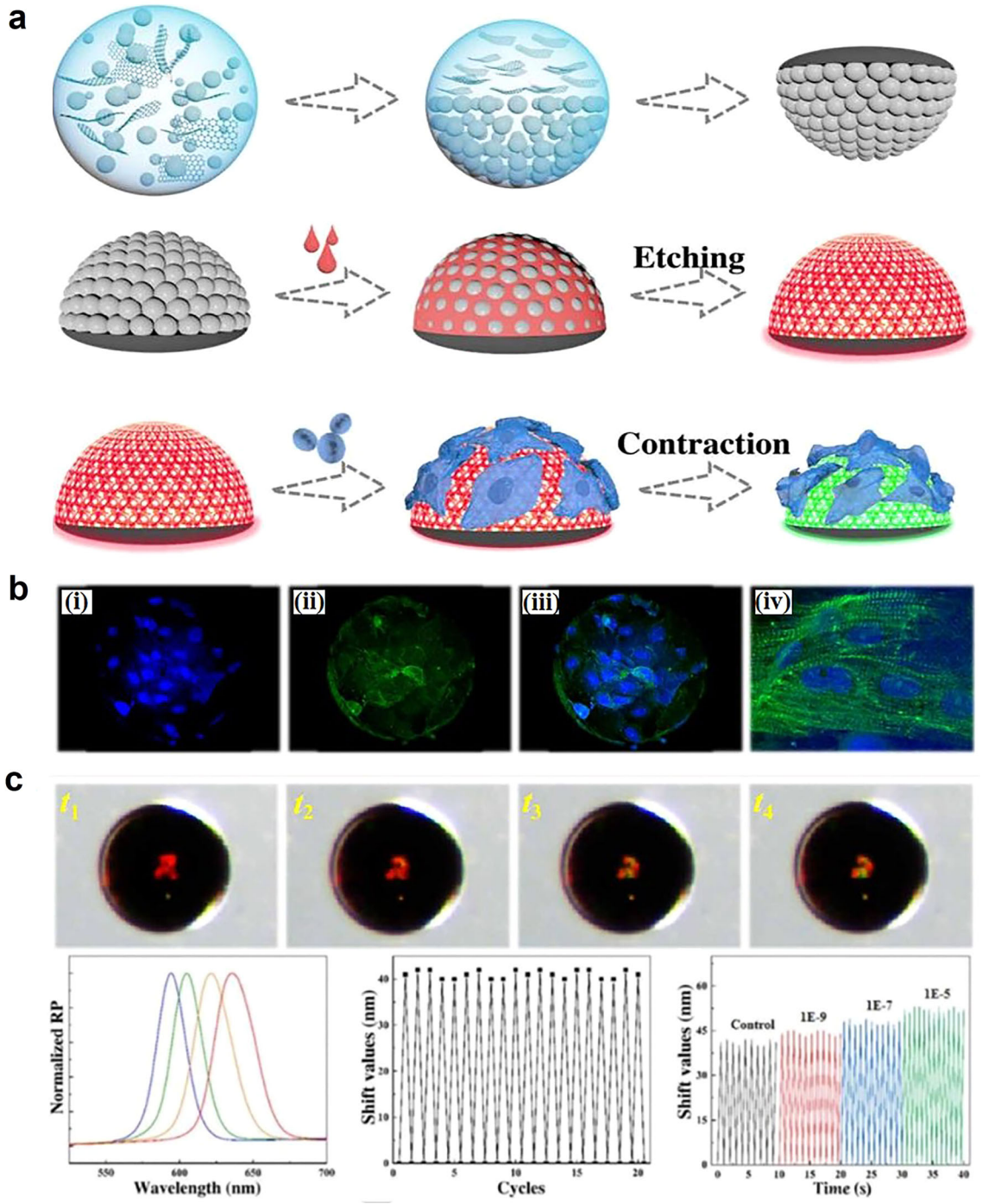

Fig. 12 **a** Schematic diagrams of the preparation process and cardiomyocyte detecting of the anisotropic Janus beads; **b** fluorescence images of the cardiomyocytes cultured on a hydrogel bead; **c** the hydrogel beads for self-reporting drug testing [78]

and explore more intuitive and efficient strategies. Taking inspiration from natural creatures with bright structural color, natural PhC materials are carefully investigated and thus multiform synthetic PhC materials occurred. For different PhC materials, their optical features have been well utilized to impart them with novel and excellent biosensing capabilities, which provide a novel approach to realize visual structural color feedback for cellular environment, such as temperature, pH, cell activity. Besides optical properties, the porous structures of PhCs also possess biological value, leading to an extensive application in tissue engineering and drug release. These characteristics suggest the potential of PhC materials in heart-on-chips, so that scientists have devoted themselves to implement practical applications. We herein analyze the

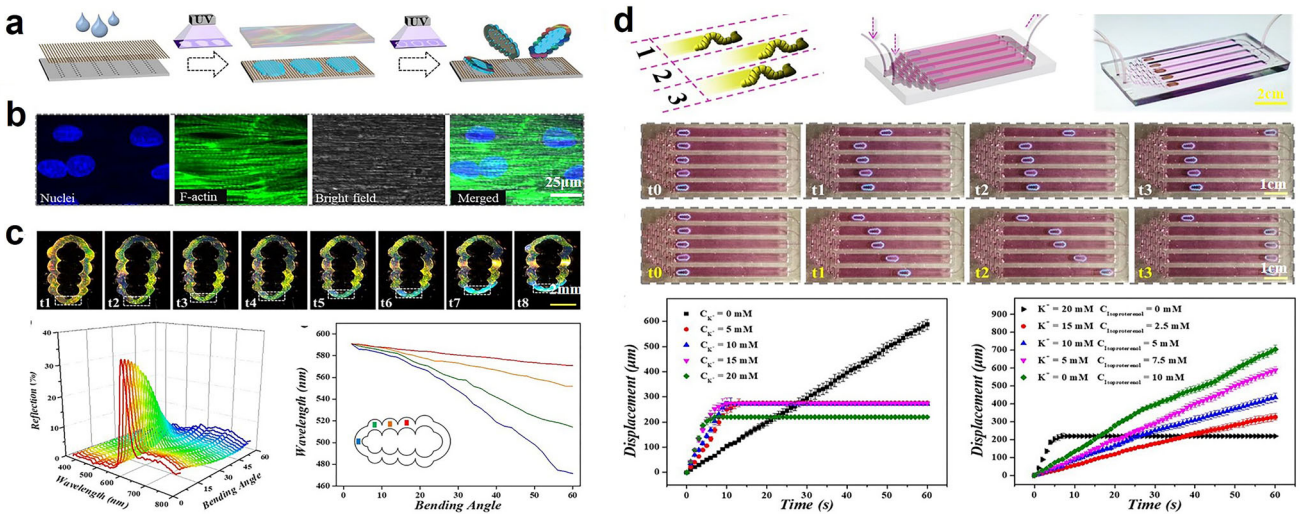

Fig. 13 **a** Schematic diagram of the generation process of the caterpillar-like soft robot; **b** fluorescent images of the cardiomyocytes cultured on CNT-coated hydrogel; **c** the color variation during the movement process of the soft robot; **d** the integration of soft robots in a microfluidic heart-on-chip system [79]

inherent properties and the derived applications in mimicking extracellular matrix and fabricating PhC material-based optical sensors, and then review the construction of visualized heart-on-chips based on PhC materials.

Although the researches of PhC materials in heart-on-chips have made a significant progress in recent years, there remain challenges and limitations for further development. The heart-on-chips integrated with hydrogels possessed self-reporting feedback. However, these chips constructed with non-human cells could not adequately represent human biology and might show significant differences in drug response and disease mechanisms. Thus, it is necessary to develop strategies to establish in vitro systems with better human biological simulation and drug-induced toxicity analysis. With the improved functions, the self-reporting heart-on-chips are expected to execute more complicated functions and applications in physiological imitation and clinical treatments. We believe that the abilities of PhCs-based heart-on-chips to detect myocardial mechanics and give visualized response would shine brilliantly in the disease treatment and diagnosis in the future.

Acknowledgements This work was supported by the National Natural Science Foundation of China (Grants 61927805), the Natural Science Foundation of Jiangsu (Grant No. BE2018707) and the Scientific Research Foundation of Nanjing University and Drum Tower Hospital.

Compliance with ethical standards

Conflict of interest The authors declare that they have no conflict of interest.

Human and animal rights This review does not contain any studies with human or animal subjects performed by any of the authors.

References

1. Huh D, Matthews BD, Mammoto A, Montoya-Zavala M, Hsin HY, Ingber DE (2010) Reconstituting organ-level lung functions on a chip. Science 328:1662–1668. https://doi.org/10.1126/science.1188302
2. Huh D, Fujioka H, Tung YC, Futai N, Paine R, Grotberg JB, Takayama S (2007) Acoustically detectable cellular-level lung injury induced by fluid mechanical stresses in microfluidic airway systems. Proc Natl Acad Sci USA 104:18886–18891. https://doi.org/10.1073/pnas.0610868104
3. Huh D, Leslie DC, Matthews BD et al (2012) A human disease model of drug toxicity–induced pulmonary edema in a lung-on-a-chip microdevice. Sci Transl Med 4:159ra147. https://doi.org/10.1126/scitranslmed.3004249
4. Perestrelo AR, Águas AC, Rainer A, Forte G (2015) Microfluidic organ/body-on-a-chip devices at the convergence of biology and microengineering. Sensors 15:31142–31170. https://doi.org/10.3390/s151229848
5. Park SE, Georgescu A, Huh D (2019) Organoids-on-a-chip. Science 364:960–965. https://doi.org/10.1126/science.aaw7894
6. Piccini JP, Whellan DJ, Berridge BR et al (2009) Current challenges in the evaluation of cardiac safety during drug development: translational medicine meets the critical path initiative. Am Heart J 158:317–326. https://doi.org/10.1016/j.ahj.2009.06.007
7. Shah RR (2006) Can pharmacogenetics help rescue drugs withdrawn from the market? Future Med. https://doi.org/10.2217/14622416.7.6.889
8. Kurokawa YK, George SC (2016) Tissue engineering the cardiac microenvironment: multicellular microphysiological systems for drug screening. Adv Drug Deliv Rev 96:225–233. https://doi.org/10.1016/j.addr.2015.07.004
9. Mathur A, Loskill P, Shao K, Huebsch N, Hong S, Marcus SG, Marks N, Mandegar M, Conklin BR, Lee LP, Healy KE (2015) Human iPSC-based cardiac microphysiological system for drug

screening applications. Sci Rep 5:8883. https://doi.org/10.1038/srep08883
10. Yesil-Celiktas O, Hassan S, Miri AK, Maharjan S, Al-kharboosh R, Quiñones-Hinojosa A, Zhang YS (2018) Mimicking human pathophysiology in organ-on-chip devices. Adv Biosyst 2:1800109. https://doi.org/10.1002/adbi.201800109
11. Zhang YS, Aleman J, Shin SR et al (2017) Multisensor-integrated organs-on-chips platform for automated and continual in situ monitoring of organoid behaviors. Proc Natl Acad Sci USA 114:E2293–E2302. https://doi.org/10.1073/pnas.1612906114
12. Shin SR, Kilic T, Zhang YS et al (2017) Label-free and regenerative electrochemical microfluidic biosensors for continual monitoring of cell Secretomes. Adv Sci 4:1600522. https://doi.org/10.1002/advs.201600522
13. Boudou T, Legant WR, Mu A et al (2012) A microfabricated platform to measure and manipulate the mechanics of engineered cardiac microtissues. Tissue Eng Part A 18:910–919. https://doi.org/10.1089/ten.tea.2011.0341
14. Grosberg A, Alford PW, McCain ML, Parker KK (2011) Ensembles of engineered cardiac tissues for physiological and pharmacological study: heart on a chip. Lab Chip 11:4165–4173. https://doi.org/10.1039/C1LC20557A
15. Wang L, Dou W, Malhi M et al (2018) Microdevice platform for continuous measurement of contractility, beating rate, and beating rhythm of human-induced pluripotent stem cell-cardiomyocytes inside a controlled incubator environment. ACS Appl Mater Interfaces 10:21173–21183. https://doi.org/10.1021/acsami.8b05407
16. Polacheck WJ, Chen CS (2016) Measuring cell-generated forces: a guide to the available tools. Nat Methods 13:415. https://doi.org/10.1038/nmeth.3834
17. Lind JU, Busbee TA, Valentine AD et al (2017) Instrumented cardiac microphysiological devices via multimaterial three-dimensional printing. Nat Mater 16:303–308. https://doi.org/10.1038/nmat4782
18. Yoon J, Eyster TW, Misra AC, Lahann J (2015) Cardiomyocyte-driven actuation in biohybrid microcylinders. Adv Mater 27:4509–4515. https://doi.org/10.1002/adma.201501284
19. Kang Y, Walish JJ, Gorishnyy T, Thomas EL (2007) Broad-wavelength-range chemically tunable block-copolymer photonic gels. Nat Mater 6:957–960. https://doi.org/10.1038/nmat2032
20. Ge D, Lee E, Yang L, Cho Y, Li M, Gianola DS, Yang S (2015) A robust smart window: reversibly switching from high transparency to angle-independent structural color display. Adv Mater 27:2489–2495. https://doi.org/10.1002/adma.201500281
21. Yue Y, Kurokawa T, Haque MA et al (2014) Mechano-actuated ultrafast full-colour switching in layered photonic hydrogels. Nat Commun 5:1–8. https://doi.org/10.1038/ncomms5659
22. Phillips KR, England GT, Sunny S, Shirman E, Shirman T, Vogel N, Aizenberg J (2016) A colloidoscope of colloid-based porous materials and their uses. Chem Soc Rev 45:281–322. https://doi.org/10.1039/C5CS00533G
23. Yang D, Ye S, Ge J (2014) From metastable colloidal crystalline arrays to fast responsive mechanochromic photonic gels: an organic gel for deformation-based display panels. Adv Funct Mater 24:3197–3205. https://doi.org/10.1002/adfm.201303555
24. Kolle M, Zheng B, Gibbons N, Baumberg JJ, Steiner U (2010) Stretch-tuneable dielectric mirrors and optical microcavities. Opt Exp 18:4356–4364. https://doi.org/10.1364/OE.18.004356
25. Park TH, Yu S, Cho SH et al (2018) Block copolymer structural color strain sensor. NPG Asia Mater 10:328–339. https://doi.org/10.1038/s41427-018-0036-3
26. Diao YY, Liu XY, Toh GW, Shi L, Zi J (2013) Multiple structural coloring of silk-fibroin photonic crystals and humidity-responsive color sensing. Adv Funct Mater 23:5373–5380. https://doi.org/10.1002/adfm.201203672
27. Yablonovitch E (1987) Inhibited spontaneous emission in solid-state physics and electronics. Phys Rev Lett 58:2059. https://doi.org/10.1103/PhysRevLett.58.2059
28. John S (1987) Strong localization of photons in certain disordered dielectric superlattices. Phys Rev Lett 58:2486. https://doi.org/10.1103/PhysRevLett.58.2486
29. Sun J, Bhushan B, Tong J (2013) Structural coloration in nature. RSC Adv 3:14862–14889. https://doi.org/10.1039/C3RA41096J
30. Cong H, Yu B, Tang J, Li Z, Liu X (2013) Current status and future developments in preparation and application of colloidal crystals. Chem Soc Rev 42:7774–7800. https://doi.org/10.1039/C3CS60078E
31. Zhao Y, Xie Z, Gu H, Zhu C, Gu Z (2012) Bio-inspired variable structural color materials. Chem Soc Rev 41:3297–3317. https://doi.org/10.1039/c2cs15267c
32. Davis KE, Russel WB, Glantschnig WJ (1991) Settling suspensions of colloidal silica: observations and X-ray measurements. J Chem Soc, Faraday Trans 87:411–424. https://doi.org/10.1039/FT9918700411
33. Denkov ND, Velev OD, Kralchevsky PA, Ivanov IB, Yoshimura H, Nagayama K (1993) Two-dimensional crystallization. Nature 361:26. https://doi.org/10.1038/361026a0
34. Jiang P, Bertone JF, Hwang KS, Colvin VL (1999) Single-crystal colloidal multilayers of controlled thickness. Chem Mater 11:2132–2140. https://doi.org/10.1021/cm990080+
35. Yang H, Jiang P (2010) Large-scale colloidal self-assembly by doctor blade coating. Langmuir 26:13173–13182. https://doi.org/10.1021/la101721v
36. Gu ZZ, Fujishima A, Sato O (2002) Fabrication of high-quality opal films with controllable thickness. Chem Mater 14:760–765. https://doi.org/10.1021/cm0108435
37. Zhao Y, Shang L, Cheng Y, Gu Z (2014) Spherical colloidal photonic crystals. Acc Chem Res 47:3632–3642. https://doi.org/10.1021/ar500317s
38. Zhao Y, Zhao X, Sun C, Li J, Zhu R, Gu Z (2008) Encoded silica colloidal crystal beads as supports for potential multiplex immunoassay. Anal Chem 80:1598–1605. https://doi.org/10.1021/ac702249a
39. Wang JT, Wang J, Han JJ (2011) Fabrication of advanced particles and particle—based materials assisted by droplet—based microfluidics. Small 7:1728–1754. https://doi.org/10.1002/smll.201001913
40. Kim SH, Jeon SJ, Yi GR, Heo CJ, Choi JH, Yang SM (2008) Optofluidic assembly of colloidal photonic crystals with controlled sizes, shapes, and structures. Adv Mater 20:1649–1655. https://doi.org/10.1002/adma.200703022
41. Ge J, Lee H, He L et al (2009) Magnetochromatic microspheres: rotating photonic crystals. J Am Chem Soc 131:15687–15694. https://doi.org/10.1021/ja903626h
42. Srinivas RL, Chapin SC, Doyle PS (2011) Aptamer-functionalized microgel particles for protein detection. Anal Chem 83:9138–9145. https://doi.org/10.1021/ac202335u
43. Kanai T, Lee D, Shum HC, Weitz DA (2010) Fabrication of tunable spherical colloidal crystals immobilized in soft hydrogels. Small 6:807–810. https://doi.org/10.1002/smll.200902314
44. Xu Y, Wang H, Chen B, Liu H, Zhao Y (2019) Emerging barcode particles for multiplex bioassays. Sci China Mater 62:89–324. https://doi.org/10.1007/s40843-018-9330-5
45. Choi SW, Zhang Y, Thomopoulos S, Xia Y (2010) In vitro mineralization by preosteoblasts in poly (DL-lactide-co-glycolide) inverse opal scaffolds reinforced with hydroxyapatite nanoparticles. Langmuir 26:12126–12131. https://doi.org/10.1021/la101519b
46. Zhang YS, Regan KP, Xia Y (2013) Controlling the pore sizes and related properties of inverse opal scaffolds for tissue engineering applications. Macromol Rapid Commun 34:485–491. https://doi.org/10.1002/marc.201200740

47. Choi SW, Xie J, Xia Y (2009) Chitosan-based inverse opals: three-dimensional scaffolds with uniform pore structures for cell culture. Adv Mater 21:2997–3001. https://doi.org/10.1002/adma.200803504
48. Zhang YS, Zhu C, Xia Y (2017) Inverse opal scaffolds and their biomedical applications. Adv Mater 29:1701115. https://doi.org/10.1002/adma.201701115
49. Wang J, Chen G, Zhao Z, Sun L, Zou M, Ren JA, Zhao Y (2018) Responsive graphene oxide hydrogel microcarriers for controllable cell capture and release. Sci China Mater 61:1314–1324. https://doi.org/10.1007/s40843-018-9251-9
50. He J, Sun C, Gu Z et al (2018) Morphology, migration, and transcriptome analysis of schwann cell culture on butterfly wings with different surface architectures. ACS Nano 12:9660–9668. https://doi.org/10.1021/acsnano.8b00552
51. Elbaz A, Lu J, Gao B, Zheng F, Mu Z, Zhao Y, Gu Z (2017) Chitin-based anisotropic nanostructures of butterfly wings for regulating cells orientation. Polymers 9:386. https://doi.org/10.3390/polym9090386
52. Dong C, Lv Y (2016) Application of collagen scaffold in tissue engineering: recent advances and new perspectives. Polymers 8:42. https://doi.org/10.3390/polym8020042
53. Dvir T, Timko BP, Kohane DS, Langer R (2011) Nanotechnological strategies for engineering complex tissues. Nat Nanotechnol 6:13. https://doi.org/10.1038/nnano.2010.246
54. Engel E, Michiardi A, Navarro M, Lacroix D, Planell JA (2008) Nanotechnology in regenerative medicine: the materials side. Trends Biotechnol 26:39–47. https://doi.org/10.1016/j.tibtech.2007.10.005
55. Sell SA, Wolfe PS, Garg K, McCool JM, Rodriguez IA, Bowlin GL (2010) The use of natural polymers in tissue engineering: a focus on electrospun extracellular matrix analogues. Polymers 2:522–553. https://doi.org/10.3390/polym2040522
56. Ding Y, Sun J, Ro HW et al (2011) Thermodynamic underpinnings of cell alignment on controlled topographies. Adv Mater 23:421–425. https://doi.org/10.1002/adma.201001757
57. Lee YS, Livingston AT (2011) Electrospun nanofibrous materials for neural tissue engineering. Polymers 3:413–426. https://doi.org/10.3390/polym3010413
58. Schulte VA, Díez M, Möller M, Lensen MC (2009) Surface topography induces fibroblast adhesion on intrinsically nonadhesive poly (ethylene glycol) substrates. Biomacromol 10:2795–2801. https://doi.org/10.1021/bm900631s
59. Lu H, Feng Z, Gu Z, Liu C (2009) Growth of outgrowth endothelial cells on aligned PLLA nanofibrous scaffolds. J Mater Sci Mater Med 20:1937–1944. https://doi.org/10.1007/s10856-009-3744-y
60. Zhang Z, Cui H (2012) Biodegradability and biocompatibility study of poly (chitosan-g-lactic acid) scaffolds. Molecules 17:3243–3258. https://doi.org/10.3390/molecules17033243
61. Park S, Park KM (2016) Engineered polymeric hydrogels for 3D tissue models. Polymers 8:23. https://doi.org/10.3390/polym8010023
62. Wang YC, Tang ZM, Feng ZQ, Xie ZY, Gu ZZ (2010) Stretched inverse opal colloid crystal substrates-induced orientation of fibroblast. Biomed Mater 5:035011. https://doi.org/10.1088/1748-6041/5/3/035011
63. Lu J, Zou X, Zhao Z, Mu Z, Zhao Y, Gu Z (2015) Cell orientation gradients on an inverse opal substrate. ACS Appl Mater Interfaces 7:10091–10095. https://doi.org/10.1021/acsami.5b02835
64. Fattahi P, Borhan A, Abidian MR (2013) Microencapsulation: microencapsulation of chemotherapeutics into monodisperse and tunable biodegradable polymers via electrified liquid jets: control of size, shape, and drug release. Adv Mater 25:4529. https://doi.org/10.1002/adma.201370205
65. Zhang B, Cheng Y, Wang H, Ye B, Shang L, Zhao Y, Gu Z (2015) Multifunctional inverse opal particles for drug delivery and monitoring. Nanoscale 7:10590–10594. https://doi.org/10.1039/C5NR02324F
66. Zhang H, Liu D, Wang L et al (2017) Microfluidic encapsulation of prickly zinc-doped copper oxide nanoparticles with VD1142 modified spermine acetalated dextran for efficient cancer therapy. Adv Healthc Mater 6:1601406. https://doi.org/10.1002/adhm.201601406
67. Zhang H, Liu Y, Wang J, Shao C, Zhao Y (2019) Tofu-inspired microcarriers from droplet microfluidics for drug delivery. Sci China Chem 62:87–94. https://doi.org/10.1007/s11426-018-9340-y
68. Liu Y, Shao C, Bian F, Yu Y, Wang H, Zhao Y (2018) Egg component-composited inverse opal particles for synergistic drug delivery. ACS Appl Mater Interfaces 10:17058–17064. https://doi.org/10.1021/acsami.8b03483
69. Ueno K, Matsubara K, Watanabe M, Takeoka Y (2007) An electro- and thermochromic hydrogel as a full-color indicator. Adv Mater 19:2807–2812. https://doi.org/10.1002/adma.200700159
70. Wang T, Liu J, Nie F (2018) Non-dye cell viability monitoring by using pH-responsive inverse opal hydrogels. J Mater Chem B 6:1055–1065. https://doi.org/10.1039/C7TB02631E
71. Chen Z, Fu F, Yu Y, Wang H, Shang Y, Zhao Y (2019) Cardiomyocytes-actuated Morpho butterfly wings. Adv Mater 31:1805431. https://doi.org/10.1002/adma.201805431
72. Fu F, Shang L, Chen Z, Yu Y, Zhao Y (2018) Bioinspired living structural color hydrogels. Sci Robot 3:eaar8580. https://doi.org/10.1126/scirobotics.aar8580
73. Li LJ, Chen ZY, Shao CM, Sun LY, Sun LY, Zhao YJ (2020) Graphene hybrid anisotropic structural color film for cardiomyocytes' monitoring. Adv Funct Mater 30:1906353. https://doi.org/10.1002/adfm.201906353
74. Shang Y, Chen Z, Fu F et al (2018) Cardiomyocyte-driven structural color actuation in anisotropic inverse opals. ACS Nano 13:796–802. https://doi.org/10.1021/acsnano.8b08230
75. Choi TM, Park JG, Kim YS, Manoharan VN, Kim SH (2015) Osmotic-pressure-mediated control of structural colors of photonic capsules. Chem Mater 27:1014–1020. https://doi.org/10.1021/cm5043292
76. Shang L, Cheng Y, Zhao Y (2017) Emerging droplet microfluidics. Chem Rev 117:7964–8040. https://doi.org/10.1021/acs.chemrev.6b00848
77. Wang H, Gu H, Chen Z, Shang L, Zhao Z, Gu Z, Zhao Y (2017) Enzymatic inverse opal hydrogel particles for biocatalyst. ACS Appl Mater Interfaces 9:12914–12918. https://doi.org/10.1021/acsami.7b01866
78. Wang H, Liu Y, Chen Z, Sun L, Zhao Y (2020) Anisotropic structural color particles from colloidal phase separation. Sci Adv 6:eaay1438. https://doi.org/10.1126/sciadv.aay1438
79. Sun L, Chen Z, Bian F, Zhao Y (2020) Bioinspired soft robotic caterpillar with cardiomyocyte drivers. Adv Funct Mater 30:1907820. https://doi.org/10.1002/adfm.201907820